Detonation Initiation by Reflection of a Fast-Flame at an Obstacle

Maddy Moran and Gaby Ciccarelli
Queen's University
Kingston, Ontario, Canada

1 Introduction

For deflagration-to-detonation transition (DDT) to occur, the flame must reach the combustion product's speed of sound, forming a shock-flame complex (fast-flame). Lateral confinement and turbulence from obstructions enable such acceleration [1]. This phenomenon is often studied in cylindrical tubes with orifice plates [2]. Mehr and Ciccarelli [3] found that in this setup, DDT is driven by shock reflection from the orifice plate. Detonation transmits through the plate when the detonation cell size (λ) meets $d < 13\lambda$; otherwise, the wave decouples due to diffraction. The decoupled shock and turbulent flame can interact with subsequent orifice plates, potentially triggering detonation. Shock interaction with obstacles is crucial for both DDT and detonation propagation in obstructed channels.

Voevodsky and Soloukhin [4] performed normal shock reflection experiments with $2H_2+O_2$ and observed two detonation initiation modes; at high reflected shock temperatures, a single ignition site was observed (strong ignition), while lower reflected shock temperatures resulted in multiple ignition sites which merged to form a detonation away from the wall (mild ignition). Meyer and Oppenheim [5] used schlieren photography to visualize their planar shock reflection experiment. They observed strong and weak detonation initiation and showed that ignition at the highest reflected shock temperatures was uniform at the end wall, producing a planar detonation that overtakes the reflected shock wave. At lower reflected shock temperatures, a loci of ignition sites at the end wall (coined mild ignition in [4]) resulted in flame acceleration and subsequent transition to detonation. They proposed a criterion based on chemical kinetics to define the transition between weak and strong detonation initiation. Thomas et al. [6] investigated planar shock reflection at an obstacle and concluded that larger incident shock Mach numbers were required for detonation initiation compared to the wall reflection case, and this discrepancy was credited to the expansion of the doubly-shocked gas next to the obstacle. They proposed a detonation initiation limit that considered the ratio of the chemical reaction time scale evaluated at reflected shock temperature and pressure and the transit time for an acoustic wave to travel down the obstacle face. Recently, in similar shock tube experiments Yousefi Asli Mozhdehe et al. [7] observed a new weak detonation initiation mechanism which occurs in reflected shock bifurcation stagnation bubble. Chan et al. [8] studied detonation initiation with $2H_2+O_2$ where a Mach stem interacts with a 2.54 cm obstacle. The critical Mach number for strong initiation ranged from 2.5 – 2.8. The initiation process when a steady-state Mach stem collided with an obstacle mounted on a variable angle ramp was

Correspondence to: gaby.ciccarelli@queensu.ca

also examined and a critical post-incident shock temperature of 1150 K was required for strong detonation initiation.

The objective of the current study is to examine the interaction of a shock-flame complex with an obstacle. The shock-flame complex is produced via diffraction of a fast-flame at a back-facing step, simulating the obstacle-laden channel experiment while removing the variability and strength of the shock-flame complex as it diffracts at each obstacle. The obstacle height was varied and the effect of the trailing flame in enhancing or mitigating detonation initiation was investigated.

2 Experimental set-up

A test channel composed of four sections arranged in series was used to investigate the interaction of a fast-flame with an obstacle after it diffracts over a back-facing step, see Fig. 1. The first section, consisting of a 1.22 m long, 7.6 cm inner-diameter round tube with repeating 50% blockage ratio orifice plates spaced at 7.6 cm, was used to generate a detonation wave. A spark plug mounted on the endplate was used for ignition of the mixture at various sub-atmospheric initial pressures. The detonation exiting the round tube section stabilized in an obstacle-free 61 cm long, 7.6 cm square cross-section. The third section was also 61 cm long, and 7.6 cm square cross-section and housed a porous plate 15 cm downstream from the beginning of the section. The porous plate, consisting of thirty-six uniformly distributed 6.4 mm diameter holes, quenched the detonation producing a fast-flame.

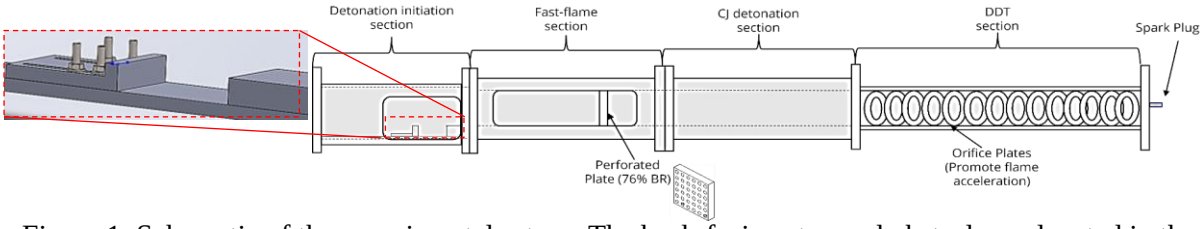

Figure 1: Schematic of the experimental set-up. The back-facing step and obstacle are located in the final test section. An isometric view of the channel configuration is also provided.

The final 12.7 cm by 7.6 cm rectangular test section had a 2.54 cm tall back-facing step followed by a 12.7 cm thick fence-type obstacle that spanned across the channel width where detonation initiation occurs. The test section was configured such the obstacle was located 11.43 cm downstream from the back-facings step, and three obstacle heights (2.54 cm and 3.81 cm) were used in experiments. This section was equipped with two acrylic windows on either side through which schlieren video was recorded. The schlieren system included a 25.4 cm diameter parabolic mirror and either a Shimadzu HPV-X2 or Photron SAZ camera to capture the diffraction of the fast-flame and subsequent interaction with the obstacle. 0.5 mm aluminium soot-coated foils were used on the channel floor and rear window of this section to record the cell structure evolution of the detonation initiation event. The consistency of the flame profile as it enters the test section and diffracts over the back-facing step was examined by capturing the flame chemiluminescence via regular photography at a 45-degree angle to the channel axis. The shock velocity was measured by dividing the distance travelled in three consecutive schlieren video frames by the elapsed time before shock collision with the obstacle, the spatial resolution resulted in a 3% uncertainty in the measurement. The experiment was performed with two different mixtures; $2H_2 + O_2$ to compare to Mach stem reflection studies in [8], and $C_2H_4 + 3O_2 + 3N_2$ to compare to wall and obstacle reflection studies in [7]. Limited tests with a 1.27 cm tall obstacle at a stand-off position of 15.2 cm were performed with $2H_2 + O_2$ for a complete comparison of the present study with [8]. The initial pressure was varied from 15 kPa – 24 kPa such that the incident shock velocity upstream from the back-facing step was altered.

3 Results and Discussion

3.1. Detonation initiation mechanism

Schlieren photography for both mixtures regardless of obstacle height was similar, so only the results for $2H_2 + O_2$ will be described. Figure 2a shows select schlieren video frames showing strong detonation initiation for $2H_2 + O_2$ at an initial pressure of 20 kPa (obstacle height: 2.54 cm). The incident shock (I) reflection off the channel floor develops a transverse-reflected shock (T) and Mach stem perpendicular to the bottom wall; also evident in images 1 and 2 is the shear layer coming off the triple point that curls at the floor in image 2. The Mach stem increases in height as it propagates, and upon collision with the obstacle it is ~1.25 cm tall (roughly half the obstacle height). For this test, the Mach number of the Mach stem was calculated to be 2.7. Due to the higher speed of sound in the combustion products compared to that of the post-incident shock, the reflected-transverse wave "bends" as it crosses the flame. Between images 2 and 3, the Mach stem reflects normally off the obstacle and detonation initiation at the obstacle face below the height of the triple point collision follows. The detonation front is visible in image 4, and it is evident that the initiation event occurs before the obstacle-reflected shock encounters the flame. The detonation front diffracts around the obstacle's external corner (see arrow in image 5) and the part of the detonation front that crosses the flame will continue as a shock wave (arrow in image 6).

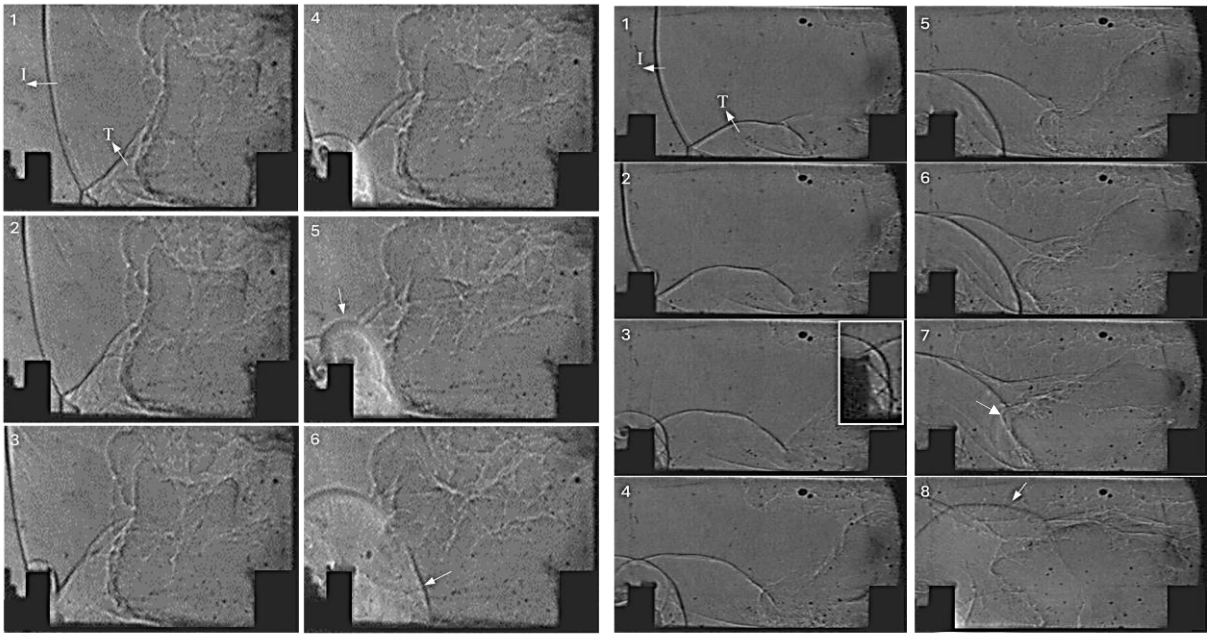

Figure 2: $2H_2 + O_2$ schlieren frames with 2.54 cm obstacle configuration showing (a) Strong detonation initiation (P_i = 20 kPa, M_s = 2.7, 7 μs between frames). (b) Detonation initiation via shock-flame interaction (P_i = 17 kPa, M_s = 2.4, 15 μs between frames). A zoomed-in view of the obstacle face interaction is provided in image 3.

Detonation initiation via shock-flame interaction for $2H_2 + O_2$ at an initial pressure of 17 kPa (obstacle height: 2.54 cm) is depicted in the select schlieren video frames provided in Fig. 2b. The gap between the shock and the flame is more significant as compared to the strong initiation test shown in Fig. 2a. Image 2 shows the instance the Mach stem collides with the obstacle. The curved reflected shock generated at the top external corner of the obstacle due to the obstacle-incident shock interaction is also seen in image 2. The Mach number of the Mach stem, measured from sequential video frames, is determined to be 2.4, compared to 2.7 in the test for Fig. 2a. Upon normal reflection of the Mach stem, detonation initiation does not occur, consequently, more details of the incident shock reflection off the obstacle are observed. Particularly, in image 3 the reflected shock generated at the obstacle's external corner travels down the obstacle face while the transverse-reflected shock propagates up the face (see zoomed-in image inset). The obstacle external corner reflection generates high pressure that mitigates

the progressive cooling of the expansion fan down the obstacle face following normal shock reflection [6, 7]. The propagation of the obstacle-reflected shock as it approaches the flame is observed in images 5 and 6. Also seen in these images is the uneventful interaction of the transverse-reflected shock with the flame that occurs significantly further upstream compared to Fig. 2a due to the larger initial gap between the shock and flame upon entering the test section. Detonation initiation occurs due to the interaction of the obstacle-reflected shock and the flame, between images 6 and 7. In image 8, a curved detonation (see arrow) is observed which can be tracked back to a bright spot appearing in image 7 (see arrow) that is surrounded by what could be interpreted as a detonation kernel originating at a point on the flame surface. Unaffected parts of the flame are still observed in image 7 because the channel width is much larger than the detonation kernel and schlieren integrates across the entire width.

3.2. Detonation initiation mechanism

Strong detonation initiation resulted from the normal reflection of the Mach stem from the obstacle face. SD Toolbox [9] with the 'Sandiego' mechanism was used to calculate the normal reflected shock state. Figure 3 summarizes the detonation initiation data for (a) $2H_2 + O_2$ and (b) $C_2H_4 + 3O_2 + 3N_2$ in terms of calculated reflected shock temperature and pressure. Note that the Mach stem Mach number is provided on the upper x-axis. Strong detonation initiation corresponds to the filled-in circles, shock-flame interaction-driven initiation corresponds to the open circles, and no detonation initiation corresponds to X's. For each obstacle height, the corresponding vertical dotted line indicates the critical shock strength for strong detonation initiation. Note that there exist some outlier tests which resulted in detonation initiation via shock-flame interaction for shock Mach numbers greater than the critical value. The difference in critical shock strength for the two obstacle heights is insignificant. For $2H_2 + O_2$ the critical shock Mach number is 2.5 and the critical reflected shock temperature is ~1020 K. For $C_2H_4 + 3O_2 + 3N_2$ the critical shock Mach number is 3.1 and the critical reflected shock temperature is 1140 K. As mentioned, a larger critical Mach number for $C_2H_4 + 3O_2 + 3N_2$ is expected because it is less reactive than $2H_2 + O_2$. Shock strength was the key parameter in predicting the initiation mode, and the gap between the incident shock and flame had an insignificant effect on the initiation mode observed.

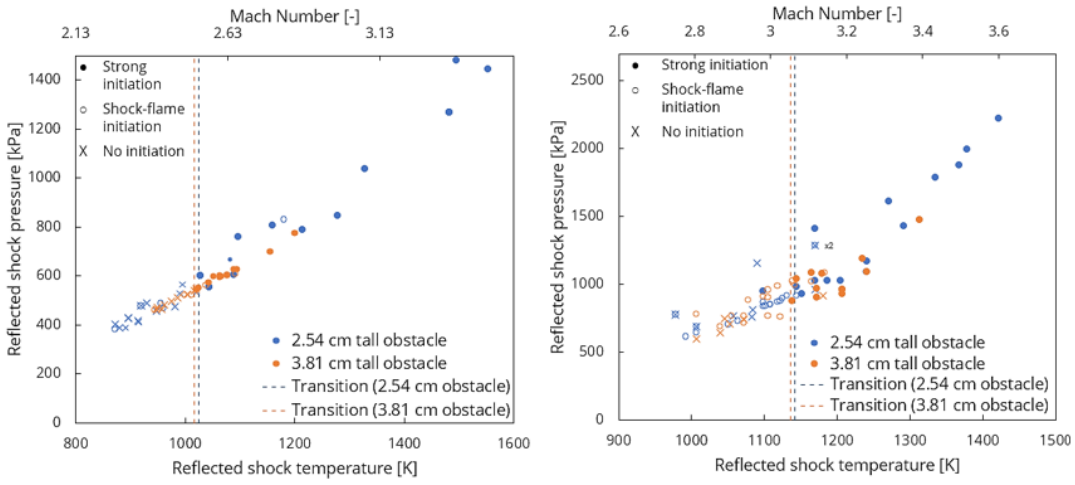

Figure 3: Detonation initiation results in terms of the calculated reflected shock temperature and pressure for (a) $2H_2 + O_2$ and (b) $C_2H_4 + 3O_2 + 3N_2$. Vertical dotted lines correspond to the critical temperature for transition between detonation initiation modes.

3.3. Mach stem detonation initiation comparison with other studies

Figure 4 compares the $2H_2 + O_2$ critical strong initiation condition for the 2.54 cm obstacle and 1.27 cm obstacle (stand-off position of 15.2 cm) from the current experiment (see Fig. 3a) to the results obtained by Chan [8]. Chan performed 15° wedge-baffle experiments with the same mixture and obstacle height. A key conclusion from experiment was that the strong initiation critical condition corresponded to a reflected shock temperature of 1150 K. Further, the critical reflected shock

temperature increased with decreasing obstacle height. In the current study, the critical Mach number for strong detonation initiation with the 2.54 cm obstacle ranged from 2.45-2.55 (blue-shaded region in Fig. 4) which corresponds to a reflected shock temperature slightly lower than 1000 K. This indicates that a weaker Mach stem is required for strong initiation in the present configuration compared to that reported in [8]. There exists an important distinction between [8] and the present study. The current experiment with the 2.54 cm obstacle configuration involves the collision of a triple point with the obstacle at approximately mid-height, i.e., the Mach stem is half the height of the obstacle; while in [8] the Mach stem height was taller than the obstacle at the time of collision. Thus, in [8] there exists an expansion wave that travels down the face of the obstacle, cooling the gas. In contrast, the present experiment involves a shock traversing the obstacle face (see inset of image 3 of Fig. 2b) that increases the temperature above the reflected shock temperature. To test this interpretation, a 1.27 cm tall obstacle was positioned at a stand-off position of 15.2 cm such that the Mach stem was taller than the obstacle upon shock reflection (see Fig. 4b), effectively replicating the shock dynamics in [8]. With this configuration, the critical Mach stem Mach number for the 1.27 cm obstacle ranged from 2.65 to 2.69, corresponding to a critical reflected shock temperature of $1125\ K\ \pm 33\ K$, see Fig. 4. This initiation condition closely matches the critical reflected shock temperature for strong initiation reported in [8].

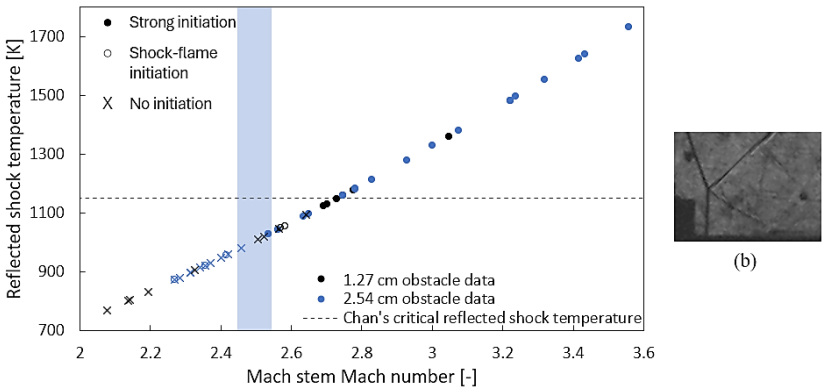

(a) (b)

Figure 4: a) Detonation initiation data for $2H_2 + O_2$ in terms of calculated reflected shock temperature versus the Mach stem Mach number for tests with a 2.54 and 1.27 cm obstacle. Transition from strong to no initiation (2.54 cm obstacle) is highlighted by a blue band. Also shown is the critical Mach stem reflected temperature of 1150 K [8]. (b) Shock-obstacle interaction with the 1.27 cm obstacle at a stand-off position of 15.2 cm.

The detonation initiation data for $C_2H_4 + 3O_2 + 3N_2$ for both obstacle heights with respect to calculated induction time and reflected shock temperature is provided in Fig. 5. The blue and orange bands on each plot correspond to the transition from strong initiation to no initiation for the 2.54 cm and 3.81 cm obstacles respectively. The red bands on each plot correspond to the transition from strong to weak detonation initiation for the reflection of a planar shock from an obstacle reported in [7]. The Thomas et. al. [6] criterion, which corresponds to the equality of the calculated reaction induction time and the acoustic transit time to travel the height of an obstacle at the reflected shock temperature, corresponds to the horizontal black dotted lines on each plot. Figure 5a shows that the critical reflected shock temperature for strong detonation initiation for the 2.54 cm obstacle ranges from 1140 – 1169 K. This is lower than the critical temperature range for the planar normal-shock reflection reported in [7] of 1223 K - 1251 K. Figure 5b shows that the critical temperature range for strong detonation initiation for the 3.81 cm obstacle is 1139 K - 1166 K. Similar to the 2.54 cm obstacle, this range is lower than the 1190 K - 1250 K range reported in [7]. Additionally, in the present experiment strong detonation initiation was observed even when the calculated induction time was longer than the acoustic transit time down the obstacle height. As previously mentioned, the reflection of the incident shock at the top external corner of the obstacle not only attenuates the generation of an expansion wave that progressively cools the gas at the obstacle face and limits strong initiation but also generates a shock that travels down the

obstacle face increasing the temperature above the Mach stem reflected temperature. Thus, an outcome of the present experiment is that strong detonation initiation is possible at a lower reflected shock temperature and longer ignition times (based on the measured Mach stem Mach number).

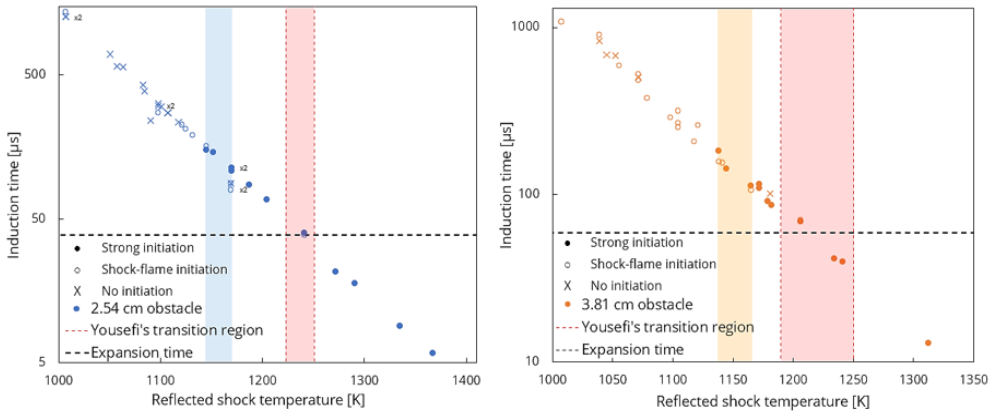

Figure 5: Detonation initiation data for $C_2H_4 + 3O_2 + 3N_2$ for the (a) 2.54 cm and (b) 3.81 cm obstacles plotted in terms of the calculated induction time versus the reflected shock temperature. The transition range from strong to weak initiation is highlighted in blue and orange, and in red for normal planar shock reflection [7].

4 Conclusions

The present experiment investigated detonation initiation via the interaction of a diffracting shock-flame complex with an obstacle. At the highest incident shock Mach numbers strong detonation initiation was observed and resulted from normal Mach stem reflection off the obstacle face. Weak detonation initiation occurred due to the interaction of the obstacle-reflected shock and the trailing flame, driven by Richtmyer-Meshkov interface instabilities. The measured strong ignition critical condition was compared with previous studies [7, 8] and it was shown that the reflected shock formed at the obstacle external corner that propagates down the obstacle face has an impact on detonation initiation. The obstacle external corner reflection produces high pressure at the top of the obstacle that mitigates the expansion that occurs for planar shock reflection [7], and for normal Mach stem reflection when the triple-point height is greater than the obstacle height [8]. This resulted in strong detonation initiation at longer ignition times and lower reflected shock temperatures.

References

[1] G. Ciccarelli and S. Dorofeev, "Flame acceleration and transition to detonation in ducts," *Prog. Energy Combust. Sci.*, vol. 34, no. 4, pp. 499–550, Aug. 2008, doi: 10.1016/j.pecs.2007.11.002.

[2] M. Cross and G. Ciccarelli, "DDT and detonation propagation limits in an obstacle filled tube," *J. Loss Prev. Process Ind.*, vol. 36, pp. 380–386, Jul. 2015, doi: 10.1016/j.jlp.2014.11.020.

[3] S. H. Mehr and G. Ciccarelli, "DDT run-up distance in an obstructed tube," *Combust. Flame*, vol. 255, p. 112906, Sep. 2023, doi: 10.1016/j.combustflame.2023.112906.

[4] V. V. Voevodsky and R. I. Soloukhin, "On the mechanism and explosion limits of hydrogen-oxygen chain self-ignition in shock waves," *Symp. Int. Combust.*, vol. 10, no. 1, pp. 279–283, Jan. 1965, doi: 10.1016/S0082-0784(65)80173-4.

[5] J. W. Meyer and A. K. Oppenheim, "On the shock-induced ignition of explosive gases," *Symp. Int. Combust.*, vol. 13, no. 1, pp. 1153–1164, Jan. 1971, doi: 10.1016/S0082-0784(71)80112-1.

[6] G. O. Thomas, S. M. Ward, R. Ll. Williams, and R. J. Bambrey, "On critical conditions for detonation initiation by shock reflection from obstacles," *Shock Waves*, vol. 12, no. 2, pp. 111–119, Aug. 2002, doi: 10.1007/s00193-002-0148-z.

[7] V. Yousefi Asli Mozhdehe, "Detonation Initiation Induced by Shock Reflection," Jan. 2024, Accessed: Feb. 13, 2024. [Online]. Available: https://hdl.handle.net/1974/32702

[8] C. K. Chan, "Collision of a shock wave with obstacles in a combustible mixture," *Combust. Flame*, vol. 100, no. 1, pp. 341–348, Jan. 1995, doi: 10.1016/0010-2180(94)00139-J.

[9] "Explosion Dynamics Laboratory." Accessed: Jan. 14, 2024. [Online]. Available: https://shepherd.caltech.edu/EDL/PublicResources/sdt/